Proceedings of ICFDP 8: ighth International Congress of Fluid Dynamics & Propulsion
December 14-17, 2006, Sharm El-Shiekh, Sinai, Egypt
ICFDP8-EG-153

THERMAL POST-BUCKLING AND FLUTTER BEHAVIOR OF SHAPE MEMORY ALLOY HYBRID COMPOSITE PLATES

Hesham Hamed Ibrahim
Space Division, National Authority for Remote Sensing and Space Sciences, Cairo, Egypt,
Hesham.ibrahim@noonrd.org

Mohammad Tawfik
Modeling and Simulation in Mechanics Department, German University in Cairo, Cairo, Egypt,
Mohammad.Tawfik@guc.edu.eg

Hani Mohammed Negm
Professor, Aerospace Engineering Department, Faculty of Engineering, Cairo University, Cairo, Egypt,
Hmnegm_cu@hotmail.com

ABSTRACT

Background. Shape memory alloys (SMAs) have a unique ability to recover large pre-strains completely when heated above certain characteristic temperature called the austenite finish temperature. During the shape recovery process, a large tensile recovery stress occurs if the SMA is restrained.

Method of Approach. In this paper, a traditional composite plate embedded with pre-strained shape memory alloy wires and subject to the combined effect of aerodynamic and thermal loading is investigated. A nonlinear finite element model based on the first order shear deformable plate theory and the von Karman strain-displacement relation is adopted to study the effectiveness of using SMA fiber embeddings on the flutter boundary, critical buckling temperature, post-buckling deflection and free vibration. The aerodynamic pressure is modeled using the quasi-steady first-order piston theory. The governing equations are obtained using the principle of virtual work based thermal strain being a cumulative physical quantity. The Newton-Raphson method is employed to obtain the post-buckling large deflection, while an Eigen value problem is solved at each temperature step to predict the free vibration frequencies about the thermally buckled equilibrium position.

Results. The numerical results show the thermal buckling, free vibrations, and flutter characteristics of shape memory alloy hybrid composites, illustrating the effect of the SMA volume fraction and pre-strain value on the aero-thermo-mechanical response of such plates.

Conclusions. It is found that the higher the volume fraction and the initial strain of the SMA fiber are, the stiffer the plate is. The critical temperature is increased and the thermal large deflection is decreased by using SMA fibers. The critical non-dimensional dynamic pressure has shown significant increase for the SMA-embedded composite plates.

Key words: Shape Memory Alloys, flutter, Thermal buckling

Nomenclature

[A], [B], [D], [As] = in-plane, coupling, bending and shear stiffness matrices of a laminate
$[A_a]$ = aerodynamic stiffness matrix
[G] = aerodynamic damping matrix
[K], [M] = system linear stiffness and mass matrices
$[K_{tan}]$ = system tangent stiffness matrix
{N}, {M}, {R} = force, moment and shear resultant vectors
[N1], [N2] = system first- and second-order nonlinear stiffness matrices
$[\overline{Q}]$ = transformed lamina reduced stiffness matrix
T_{ref} = reference temperature
V_s, V_m = volume fractions of shape memory alloy fiber and composite matrix
{W} = system nodal displacement vector
α = coefficient of thermal expansion
$\{\kappa\}$ = bending strain vector
ε_{lin} = linear strain vector
ε_{θ} = membrane nonlinear strain vector
λ = non-dimensional dynamic pressure
σ_r = recovery stress of SMA

Subscripts

b = bending
i = iteration number
m = membrane or composite matrix
r = due to recovery stress of SMA
s = static or quantity related to SMA
st = dependent on both static and dynamic displacements
t = dynamic or time dependent
x, y, z = plate Cartesian coordinates

1. INTRODUCTION

1.1. Thermal Buckling

The external skin of high speed flight vehicles experiences high temperature rise due to aerodynamic heating, which can induce thermal buckling and dynamic instability. In general, thermal buckling does not indicate structural failure. However, the thermal large deflection of the skin panels can change its aerodynamic shape causing reduction in the flight performance.

A comprehensive literature review on thermally induced flexure, buckling, and vibration of plates and shells was presented by Tauchart [1] and Thornton [2]. Shi and Mei [3] solved the problem of thermal post-buckling of composite plates with initial imperfections using the finite element modal method. The modal participation values of linear post-buckling modes were defined and used to determine the minimum number of modes needed for convergence. Gray and Mei [4] investigated the thermal post-buckling behavior and free vibrations of thermally buckled composite plates using the finite element method. The equations of motion were derived using the principle of virtual work. The temperature change over the plate is considered to be a large steady-state temperature change over the plate $\Delta T(x, y)$. Jones and Mazumdar [5] investigated the linear and non-linear dynamic behavior of plates at elevated temperatures. They presented analytical solutions for the thermal buckling and post-buckling behavior of a plate strip. A general formula is also presented which links the fundamental frequency of vibration to the critical buckling temperature and the corresponding frequency of the unheated plate. Shi et *al.* [6] investigated the thermal post-buckling behavior of symmetrically laminated and anti-symmetric angle-ply, and deflection of asymmetrically laminated composite plate under mechanical and thermal loads. A finite element formulation in modal coordinates is developed for the nonlinear thermal post-buckling of thin composite plates. The quantative contribution of each linear buckling mode shape to the post-buckling deflection was showed.

1.2. Panel Flutter

Panel flutter is a phenomenon that is usually accompanied by temperature elevation on the outer skin of high-speed air vehicles. Panel flutter is a self-excited oscillation of a plate or shell in supersonic flow. Because of aerodynamic pressure forces on the panel, two eigen modes of the structure merge and lead to this dynamic instability. Supersonic flutter of plates and shells was recognized to be an important aspect of the design of high speed vehicles when Jordan [7] observed that a number of the early V-2 rocket failures were due to panel flutter. Since then, extensive analytical and experimental research on that subject has been performed. A common remedy to the flutter problem is to stiffen those panels in danger of flutter, a method that usually introduces additional weight to the design. Thin plates are a commonly used form of structural components especially in aerospace vehicles, such as high-speed aircraft, rockets, and spacecrafts, which are subjected to thermal loads due to aerodynamic and / or solar radiation heating. This results in a temperature distribution over the surface and thermal gradient through the thickness of the plate. The presence of these thermal fields results in a flutter motion at lower dynamic pressure or a larger limit-cycle amplitude at the same dynamic pressure. Accordingly, it is important to consider the interactive effect of both aforementioned failure characteristics (flutter & thermal buckling).

A vast amount of literature exists on panel flutter using different aerodynamic theories to model the aerodynamic pressure. Mei et *al*. [8] presented a review on the various analytical methods and experimental results of supersonic and hypersonic panel flutter. Liaw [9] studied the geometrically nonlinear supersonic flutter of laminated composite thin plate structures subjected to thermal loads.. Abdel-Motagaly et *al*. [10] investigated the effect of arbitrary flow direction on the large amplitude supersonic flutter of composite panels, using the von Karman strain-displacement relation to account for large amplitude limit-cycle oscillations. The nonlinear finite element formulation introduced by Mei [11] was the basis on which Dixon and Mei [12], Xue and Mei [13], and Abdel-Motagaly et *al*. [10] built their finite element models to analyze the flutter boundaries, the limit-cycle oscillations, and the thermal problems. Dixon and Mei [12] presented a nonlinear flutter analysis of thin composite panels using finite element method. The governing equations of motion were formulated using the principle of virtual work, while the eigen value problem was solved by utilizing the linearized updated mode with nonlinear time function (LUM/NTF) approximation. Sarma and Varadan [14] studied the nonlinear flutter by using the finite element method. The governing equations were derived from energy considerations using Lagrange's equations of motion without any approximation on nonlinear terms pertaining to moderately large oscillations. Xue and Mei [13] presented an innovative finite element frequency domain solution for the nonlinear flutter response of panels under the combined effect of thermal and aerodynamic loads. Dongi et *al.* [15] investigated the nonlinear flutter of flat and slightly curved panels in high supersonic flow based on von Karman plate model and on the linear piston theory for aerodynamics. Lee et *al*. [16] performed the thermal post buckling and aerodynamic-thermal load analysis of cylindrical laminated panels using the finite element method. The panel flutter analysis under thermal stresses was carried out using Hans Krumhaar's supersonic piston theory to model aerodynamic pressure.

1.3. SMA Applications

Shape memory alloys (SMAs) have a unique ability to completely recover large pre-strains (up to 10% elongation) when heated above certain characteristic temperature called the austenite finish temperature. The austenite start temperature for Nitinol can be any where between -50 ºC and 170 ºC by varying the nickel content. During the shape recovery process, a large tensile recovery stress occurs if the SMA is restrained. Cross et *al.* [17] determined experimentally the recovery stress of Nitinol at various pre-strain valves and Young's modules versus temperatures. Both the recovery stresses and Young's modules of SMA exhibit nonlinear temperature-dependent properties. The variation of the modulus of elasticity and recovery stress of a trained Nitinol are presented in figures (1) and (2) [17].

Birman [18] presented a comprehensive review on the literature concerning SMA up to 1997. Jia and Rogers [19] formulated a mechanical model for composites with shape memory alloy embedded fibers using the micromechanical behavior of the highly nonlinear shape memory alloy and adopting the classical lamination plate theory. Park et *al.* [20] investigated the nonlinear vibration behavior of thermally buckled composite plates embedded with shape memory alloy fibers using the first order shear deformable plate theory and the von Karman strain-displacement due to large deflections. An incremental method was adopted to account for the temperature dependent material properties. Guo [21] offered an efficient finite element method for predicting the buckling temperature, post buckling deflection, and vibration characteristics for SMA hybrid composites, considering large deflection and nonlinear temperature dependent material properties of SMA. Tawfik et *al.* [22] proposed a novel concept in enhancing the thermal buckling and aeroelastic behavior of plates through embedding SMA fibers in it. He investigated the response of SMA hybrid composite plates under the combined action of aerodynamic and thermal loadings utilizing a nonlinear finite element model based on von Karman strain-displacement relation and the classical lamination plate theory. Duan et *al.* [23] presented a finite element formulation and solution procedure for free vibration behavior of SMA hybrid arbitrary laminated composite plates, taking into account temperature-dependent properties and geometrical nonlinearity. The bending displacement was separated into thermal post-buckling and small vibration at the buckled state. Roh, et *al*. [24] investigated the thermal post-buckling responses of shape memory alloy hybrid composite shell panels using a finite element method formulated on the basis of the layer wise theory and von Karman nonlinear displacement-strain relationships. The behavior of shape memory alloy wire was developed using Brinson's model [25]. Gilat and Aboudi [26] derived a micromechanically established constitutive equations for unidirectional composites with shape memory alloy fibers embedded in polymeric metallic matrices. Those equations were subsequently employed to analyze the nonlinear behavior of infinitely wide composite plates that are subjected to the sudden application of thermal loading. Guo et. *al.* [27] developed a finite element procedure to predict large amplitude nonlinear flutter response of thin Shape Memory Alloy hybrid composite plates at an arbitrary yawed angle and an elevated temperature. In this study, finite element system equations of motion are transferred to aeroelastic model coordinates to reduce the large number of structural mode degrees of freedom.

In this paper, the flutter and thermal buckling behavior of a shape memory alloy hybrid composite plate under the combined effect of thermal and aerodynamic loading are investigated using nonlinear finite element method. The nonlinear governing equations for a moderately thick rectangular plate are obtained using first-order shear-deformable plate theory (FSDT), von Karman strain-displacement relation and the principal of virtual work. The approach is based on thermal strain being a cumulative physical quantity, whereas the stress is an instant one. Thus, the thermal strain is an integral quantity of thermal expansion coefficient with respect to temperature, whereas stress is evaluated with the instant elastic modulus at a certain temperature in the thermoelastic stress-strain relations [21]. Therefore, the method does not need many small increments as in the incremental method [22], and it is suitable for any nonlinear temperature-dependent material properties. Numerical results are provided to show the effect of thermal field, SMA volume fraction and pre-strain value on the post-buckling behavior and flutter characteristics of such plates.

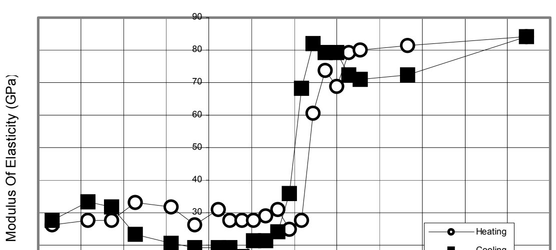

Figure 1 Variation of modulus of elasticity with temperature in heating and cooling of SMA

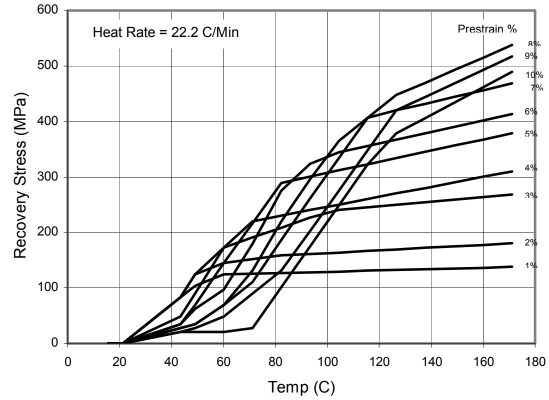

Figure 2 Recovery stress as a function of temperature and pre-strain

2. Finite Element Formulation of Thermal Post-Buckling of SMA-Embedded Plates

The equation of motion with the consideration of large deflection and temperature dependent (TD) material properties are derived for a shape memory alloy hybrid composite plate subject to aerodynamic and thermal loadings. To account for temperature dependence of material properties, a cumulative thermal strain is adopted for the calculation of the thermal deflection and stresses in the plate.

2.1. The Displacement-Nodal Displacement Relation

The degrees of freedom vector of the rectangular plate element can be written

$$\{\delta\} = \left\{ w, \phi_x, \phi_y, u, v \right\}^T = \left\{ \begin{matrix} W_b \\ W_\phi \\ W_m \end{matrix} \right\} \quad (1)$$

where w is the transverse displacement, ϕ_x and ϕ_y are the rotations of the transverse normal about the x and y axes respectively, u and v are the membrane displacements in the x and y directions respectively, $\{W_b\}$ is the transverse displacement vector, $\{W_\phi\}$ is the rotation of the transverse normal vector, and $\{W_m\}$ is the membrane displacement vector.

The displacement-nodal displacement relation can be presented in terms of interpolation function matrices $[N_w]$, $[N_u]$ and $[N_v]$ as:

$$w = [N_w]\{w_b\}^e,\ \phi_x = \left[N_{\phi_x} \right]\{W_\phi\}^e,\ \phi_y = \left[N_{\phi_y} \right]\{W_\phi\}^e, \quad (2)$$

$$u = [N_u]\{u\}^e \ \ and \ \ v = [N_v]\{v\}^e$$

where the superscript e indicates element degrees of freedom.

2.2. The Nonlinear Strain-Displacement Relation

The inplane strains and curvatures, based on von Karman large deflection and first-order shear deformable plate theory, are given by:

$$\begin{Bmatrix} \varepsilon_x \\ \varepsilon_y \\ \gamma_{xy} \end{Bmatrix} = \begin{Bmatrix} \dfrac{\partial u}{\partial x} \\ \dfrac{\partial v}{\partial y} \\ \dfrac{\partial u}{\partial y} + \dfrac{\partial v}{\partial x} \end{Bmatrix} + \begin{Bmatrix} \dfrac{1}{2}\left(\dfrac{\partial w}{\partial x}\right)^2 \\ \dfrac{1}{2}\left(\dfrac{\partial w}{\partial y}\right)^2 \\ \dfrac{\partial w}{\partial x}\dfrac{\partial w}{\partial y} \end{Bmatrix} + z\begin{Bmatrix} \dfrac{\partial \phi_y}{\partial x} \\ \dfrac{\partial \phi_x}{\partial y} \\ \dfrac{\partial \phi_y}{\partial y} + \dfrac{\partial \phi_x}{\partial x} \end{Bmatrix} \quad (3)$$

or in compact form

$$\{\varepsilon\} = \{\varepsilon_{lin}\} + \{\varepsilon_\theta\} + z\{\kappa\} \quad (4)$$

Parameters u, v and w are displacements in x, y and z directions, respectively. ε_{lin}, ε_θ, and $z\kappa$ are the membrane linear strain vector, the membrane nonlinear strain vector, and the bending strain vector, respectively.
The transverse shear strain vector can be expressed as

$$\begin{Bmatrix} \gamma_{yz} \\ \gamma_{xz} \end{Bmatrix} = \begin{Bmatrix} \phi_x \\ \phi_y \end{Bmatrix} + \begin{Bmatrix} \dfrac{\partial w}{\partial y} \\ \dfrac{\partial w}{\partial x} \end{Bmatrix} \quad (5)$$

2.3. Constitutive Equations

The composite matrix with arbitrary orientation angle θ has the principal material directions 1, 2 and 3. The SMA fiber is embedded in the 1-direction, and assumed uniformly distributed within each layer.

The material properties of the laminated composite plate embedded with SMA fibers can be written as

$$E_1 = E_{1m}V_m + E_sV_s \quad (6)$$

$$E_2 = \frac{E_{2m}E_s}{\left(E_{2m}V_s + E_sV_m\right)} \quad (7)$$

$$G_{12} = \frac{G_{12m}G_s}{\left(G_{12m}V_s + G_sV_m\right)} \quad (8)$$

$$G_{23} = G_{23m}V_m + G_sV_s \quad (9)$$

$$\nu_{12} = \nu_{12m}V_m + \nu_sV_s \quad (10)$$

$$\alpha_1 = \frac{E_{1m}\alpha_{1m}V_m + E_s\alpha_sV_s}{E_1} \quad (11)$$

$$\alpha_2 = \alpha_{2m}V_m + \alpha_sV_s \quad (12)$$

$$\rho = \rho_mV_m + \rho_sV_s \quad (13)$$

where the subscripts 'm' and 's' mean the composite matrix and SMA fiber, respectively. E, G, ν, α and ρ are Young's modulus, the shear modulus, Poisson's ratio, the thermal expansion coefficient and the material density, respectively. In addition, V_m and V_s are the volume fractions of the composite matrix and SMA fibers, respectively.

For the kth composite lamina impregnated with SMA fibers, the stress-strain relations for the FSDT can be expressed as follows [21],

$$\{\sigma\}^k = \begin{Bmatrix} \sigma_x \\ \sigma_y \\ \tau_{xy} \end{Bmatrix}^k = \left[\overline{Q}(T)\right]^k\{\varepsilon\} + \{\sigma_r(T)\}^k V_s^{\,k} - \left[\overline{Q}(T)\right]_m^k V_m^{\,k}\int_{Tref}^{T}\{\alpha(\tau)\}_m^k d\tau \quad (14)$$

$$\{\tau\}^k = \begin{Bmatrix} \tau_{yz} \\ \tau_{xz} \end{Bmatrix}^k = \begin{bmatrix} \overline{Q}_{44}(T) & \overline{Q}_{45}(T) \\ \overline{Q}_{45}(T) & \overline{Q}_{55}(T) \end{bmatrix}\begin{Bmatrix} \gamma_{yz} \\ \gamma_{xz} \end{Bmatrix} \quad (15)$$

where $\{\sigma\}$, $\{\sigma_r\}$ and $\{\tau\}$ are the inplane stress vector, the SMA recovery stress vector at the given temperature T, and the transverse shear vector, respectively. In addition, $\{\alpha\}_m$, $[\overline{Q}]$ and $[\overline{Q}]_m$ are the thermal expansion coefficient vector of the composite matrix, the transformed reduced stiffness matrix of the SMA embedded lamina, and the transformed reduced stiffness matrix of the composite matrix, respectively.

Integrating Equations (14) and (15) over the plate thickness, the constitutive equation can be obtained as

$$\begin{Bmatrix} N \\ M \end{Bmatrix} = \begin{bmatrix} A & B \\ B & D \end{bmatrix}\begin{Bmatrix} \varepsilon_m \\ \kappa \end{Bmatrix} - \begin{Bmatrix} N_T \\ M_T \end{Bmatrix} + \begin{Bmatrix} N_r \\ M_r \end{Bmatrix} \quad (16)$$

$$\{R\} = \begin{Bmatrix} R_{yz} \\ R_{xz} \end{Bmatrix} = \begin{bmatrix} A_{44} & A_{45} \\ A_{45} & A_{55} \end{bmatrix}\begin{Bmatrix} \gamma_{yz} \\ \gamma_{xz} \end{Bmatrix} = [A]^s\{\gamma\} \quad (17)$$

Where $[A]$, $[A]^s$, $[B]$ and $[D]$ are the laminate stiffness matrices, respectively. $\{N\}$, $\{M\}$ and $\{R\}$ are the resultant vectors of the inplane force, moment and transverse shear force. In addition, $\{N_T\}$ and $\{M_T\}$ are the inplane thermal load and thermal bending moment, respectively, while $\{N_r\}$ and $\{M_r\}$ are the inplane SMA recovery load and SMA recovery bending moment.

2.4. Governing Equations

By using the principle of virtual work and equations (4), (5), (16) and (17), the governing equation of thermal post-buckling and nonlinear flutter of a plate embedded with SMA fibers can be derived as follows

$$\delta W = \delta W_{int} - \delta W_{ext} = 0 \quad (18)$$

The internal virtual work δW_{int} is given as

$$\begin{aligned}\delta W_{int} &= \int_A \left(\{\delta\varepsilon_m\}^T\{N\} + \{\delta\kappa\}^T\{M\} + \{\delta\gamma\}^T\{R\}\right)dA \\ &= \{\delta W\}^T\left([K]-[K_T]+[K_r]+\frac{1}{2}[N1]+\frac{1}{3}[N2]\right)\{W\} \\ &\quad -\{\delta W\}^T\left(\{P_T\}-\{P_r\}\right)\end{aligned} \tag{19}$$

where $\{W\} = [w\,\phi_x\,\phi_y\,u\,v]$ is the displacement vector; $[K]$, $[K_T]$ and $[Kr]$ are the linear stiffness matrix, the thermal geometric stiffness matrix and the geometric stiffness matrix due to the recovery stress of the SMA fibers; $[N1]$ and $[N2]$ are the first- and second-order nonlinear stiffness matrices, respectively. In addition, $\{P_T\}$ and $\{P_r\}$ are the thermal load vector and the recovery stress load vector, respectively.

On the other hand, the external virtual work δW_{ext} is given as

$$\begin{aligned}\delta W_{ext} &= \int_A \begin{pmatrix} -I_o\left(\{\delta u\}^T\{\ddot{u}\}+\{\delta v\}^T\{\ddot{v}\}+\{\delta w\}^T\{\ddot{w}\}\right) \\ -I_2\left(\{\delta\phi_x\}^T\{\ddot{\phi}_x\}+\{\delta\phi_y\}^T\{\ddot{\phi}_y\}\right)+\{\delta w\}^T P_a\end{pmatrix} dA \\ &= -\{\delta W\}^T[M]\{\ddot{W}\} - \{\delta W_b\}^T\frac{g_a}{\omega_o}[G]\{\dot{W}_b\} \\ &\quad -\{\delta W_b\}^T\frac{\lambda}{a^3}[A_a]\{W_b\}\end{aligned} \tag{20}$$

where $(I_O, I_2) = \int_{-h/2}^{h/2} \rho\left(1, z^2\right)dz$ with h denotes the plate thickness, $[M]$ is the mass matrix, $[G]$ is the aerodynamic damping matrix, and $[A_a]$ is the aerodynamic influence matrix.

In addition,

$$P_a = -\left(\frac{g_a}{\omega_o}\frac{D_{11}}{a^4}\frac{\partial w}{\partial t} + \lambda\frac{D_{11}}{a^3}\frac{\partial w}{\partial x}\right)$$

$$q = \frac{\rho_a v^2}{2}, \qquad \beta = \sqrt{M_\infty^2 - 1}, \qquad \omega_o = \left(\frac{D_{110}}{\rho h a^4}\right)^{\frac{1}{2}},$$

$$g_a = \frac{\rho_a v\left(M_\infty^2 - 2\right)}{\rho h \omega_o \beta^3} \qquad and \qquad \lambda = \frac{2qa^3}{\beta D_{110}}$$

where P_a is the aerodynamic loading modeled using the first-order piston theory [22], v is the air flow velocity, M_∞ is the Mach number, q is the dynamic pressure, ρ_a is the air mass density, g_a is the non-dimensional aerodynamic damping, λ is the non-dimensional dynamic pressure, D_{110} is the first entry of the flexural stiffness matrix (D(1,1)), and a is the panel length.

By substituting equations (19) and (20) into (18), the governing equations for a shape memory alloy hybrid composite plate, under the combined action of aerodynamic and thermal loads, can be obtained as

$$\begin{aligned}&[M]\{\ddot{W}\}+\frac{g_a}{\omega_o}[G]\{\dot{W}\}+\left([K]-[K_T]+[K_r]+\frac{\lambda}{a^3}[A_a]+\frac{1}{2}[N1]+\frac{1}{3}[N2]\right)\{W\} \\ &=\{P_T\}-\{P_r\}\end{aligned} \tag{21}$$

3. Solution Procedures

The solution of the governing equation (21) is assumed to be as follows

$$\{W\} = \{W_s\} + \{W_t\} \tag{22}$$

where $\{W_s\}$ is the time-independent particular solution which means the large thermal deflection, and $\{W_t\}$ is the time-dependent homogenous solution. Substituting equation (22) into the governing equation (21),

$$\begin{aligned}&[M]\{\ddot{W}_t\}+\frac{g_a}{\omega_o}[G]\{\dot{W}_t\}+\left([K]-[K_T]+[K_r]+\frac{\lambda}{a^3}[A_a]\right)(\{W_s\}+\{W_t\}) \\ &+\frac{1}{2}\left([N1]_s+[N1]_t\right)(\{W_s\}+\{W_t\}) \\ &+\frac{1}{3}\left([N2]_s+[N2]_t+2[N2]_{st}\right)(\{W_s\}+\{W_t\}) \\ &=\{P_T\}-\{P_r\}\end{aligned} \tag{23}$$

Equation (23) represents the general equation for the thermal buckling and nonlinear flutter of a shape memory alloy hybrid composite plate under the combined effect of aerodynamic and thermal loads. The subscripts "s"' and "t" indicate that the relevant matrix depends on the static or dynamic displacements, respectively.

Separating static and dynamic terms of equation (23), the following two equations can be obtained [28],

$$\left([K]-[K_T]+[K_r]+\frac{\lambda}{a^3}[A_a]+\frac{1}{2}[N1]_s+\frac{1}{3}[N2]_s\right)\{W_s\}=\{P_T\}-\{P_r\} \tag{24}$$

$$\begin{aligned}&[M]\{\ddot{W}_t\}+\frac{g_a}{\omega_o}[G]\{\dot{W}_t\}+\left([K]-[K_T]+[K_r]+\frac{\lambda}{a^3}[A_a]+\frac{1}{2}[N1]_t+\frac{1}{3}[N2]_t\right)\{W_t\} \\ &+\left([N1]_s+2[N2]_{st}+[N2]_s\right)\{W_t\}=0\end{aligned} \tag{25}$$

3.1. Static Aero-thermal Buckling

The solution procedure using Newton-Raphson method for the aero-thermal post-buckling analysis of the composite plate embedded with SMA fibers is presented in the following,

Introducing the function $\{\Psi(W)\}$ to equation (24),

$$\begin{aligned}\{\Psi(W_s)\}&=\left([K]-[K_T]+[K_r]+\frac{\lambda}{a^3}[A_a]+\frac{1}{2}[N1]_s+\frac{1}{3}[N2]_s\right)\{W_s\} \\ &\quad -\{P_T\}+\{P_r\}=0\end{aligned} \tag{26}$$

Equation (26) can be written in the form of a truncated Taylor series expansion as,

$$\{\Psi(W_s+\delta W)\} = \{\Psi(W_s)\} + \frac{d\{\Psi(W_s)\}}{d(W_s)}\{\delta W\} \tag{27}$$

where

$$\frac{d\{\Psi(W_s)\}}{d(W_s)} = \left([K]-[K_T]+[K_r]+\frac{\lambda}{a^3}[A_a]+[N1]_s+[N2]_s\right) = [K_{tan}] \tag{28}$$

Thus, the Newton-Raphson iteration procedure for the determination of the post-buckling deflection can be expressed as follows:

$$\{\Psi(W_S)\}_i = \left([K]-[K_T]+[K_r]+\frac{\lambda}{a^3}[A_a]+\frac{1}{2}([N1]_S)_i+\frac{1}{3}([N2]_S)_i\right)\{W_S\} - \{P_T\}+\{P_r\}$$

$$[K_{tan}]_i\{\delta W\}_{i+1} = -\{\Psi(W_s)\}_i$$

$$\{\delta W\}_{i+1} = -[K_{tan}]^{-1}\{\Psi(W_s)\}_i$$

$$\{W_s\}_{i+1} = \{W_s\}_i + \{\delta W\}_{i+1}$$

Convergence occurs in the above procedure when the maximum value of $\{\delta W\}_{i+1}$ becomes less than a given tolerance ε_{tol}, i.e. max $|\{\delta W\}_{i+1}| \le \varepsilon_{tol}$.

3.2. Free Vibration

From equation (25), the equation of free vibration about a statically stable position can be stated as,

$$[M]\{\ddot{W}_t\}+\left([K]-[K_T]+[K_r]+\frac{\lambda}{a^3}[A_a]+[N1]_s+[N2]_s\right)\{W_t\}=0 \tag{29}$$

This can be written as,

$$[M]\{\ddot{W}_t\}+[K_{tan}]\{W_t\}=0 \tag{30}$$

Assuming the solution of the above differential equation to take the following form,

$$\{W_t\} = \bar{c}\{\Phi\}e^{\Omega t} \tag{31}$$

the generalized eigenvalue problem can be stated as,

$$\left(\Omega^2[M]+[K_{tan}]\right)\{\Phi\} = 0 \tag{32}$$

Thus, the solution procedure comprises the solution of the static thermal deflection and the associated stiffness matrices by following the procedure outlined in the preceding section, and then, solving the eigenvalue problem of equation (32) for the free vibration of a thermally buckled SMA hybrid composite plate.

3.3. Panel Flutter under Thermal Effect

In this section, the procedure of determining the critical non-dimensional dynamic pressure under the presence of thermal loading is presented. Equation (25) can be reduced for the solution of the linear (pre-buckling and pre-flutter) problem to the following equation,

$$[M]\{\ddot{W}_t\}+\frac{g_a}{\omega_o}[G]\{\dot{W}_t\} + \left([K]-[K_T]+[K_r]+\frac{\lambda}{a^3}[A_a]+[N1]_s\right)\{W_t\}=0 \tag{33}$$

Applying a new notation for the bending degree of freedom by combining the shear and bending degrees of freedom as,

$$\{W_b\} = \begin{Bmatrix} W_b \\ W_\phi \end{Bmatrix} \tag{34}$$

Separating equations (33) into membrane and transverse directions, results in the following transverse dynamic equation,

$$[M]\{\ddot{W}_b\}_t+\frac{g_a}{\omega_o}[G]\{\dot{W}_b\}_t + \left([K]-[K_T]+[K_r]+\frac{\lambda}{a^3}[A_a]+[N1_{nm}]_s\right)\{W_b\}_t=0 \tag{35}$$

Note that the terms related to *N2* and $N1_{mb}$ are dropped as they depend on W_b, which is essentially zero before buckling or flutter, while $N1_{nm}$ terms are kept as they depend on W_m which might have non-zero values depending on the boundary conditions.

Now, assuming the deflection function of the transverse displacement $\{W_b\}_t$ to be in the form ,

$$\{W_b\}_t = \bar{c}\{\Phi_b\}e^{\Omega t} \tag{36}$$

where $\Omega = \alpha + i\omega$ is the complex panel motion parameter (α is the damping ratio and ω is the frequency), $\bar{c}$ is the amplitude of vibration, and $\{\Phi_b\}$ is the mode shape.

Substituting equation (36) into (35), the generalized eigenvalue problem can be obtained as,

$$\bar{c}\left[-\kappa[\overline{M}]+[\overline{K}]\right]\{\Phi_b\}e^{\Omega t} = \{0\} \tag{37}$$

where $[\overline{M}] = \omega_o^2[M_b]$, κ is the non-dimensional eigenvalue, given by,

$$\kappa = -\left(\frac{\Omega^2}{\omega_o^2}\right) - \frac{g_a\Omega}{\omega_o} \tag{38}$$

and

$$[\overline{K}] = [K]-[K_T]+[K_r]+\frac{\lambda}{a^3}[A_a]+[N1_{nm}]_s \tag{39}$$

From equation (37) we can write the generalized eigenvalue problem,

$$\left[-\kappa[\overline{M}]+[\overline{K}]\right]\{\Phi_b\} = \{0\} \tag{40}$$

where κ is the eigenvalue and Φ_b is the mode shape, with the characteristic equation written as,

$$\left| -\kappa\left[\overline{M}\right]+\left[\overline{K}\right]\right| = \{0\} \quad (41)$$

Given that the values of κ are real for all values of λ below the critical value, an iterative solution can be utilized to determine the critical non-dimensional dynamic pressure λ_{cr}.

4. Numerical Results and Discussions

Numerical analyses for the thermal post-buckling and flutter of a laminated composite plate with and without SMA are performed using the finite element method. A uniform 6 x 6 finite element mesh of nine-noded elements is employed. The reduced order technique is used for integrating terms related to the transverse shear. In addition, 0%, 5%, 10% and 15% volume fractions and 1%, 3% and 5% initial pre-strain values of the SMA fibers are used. Results were found to have an excellent agreement with those of Ref.[21].

4.1. Aero-Thermal Buckling Analysis

Thermal post-buckling behavior of a traditional laminated composite plate with and without SMA is studied. The dimensions of the plate are 0.381 x 0.305 x 0.0013 (m) and the stacking sequence is $[0/-45/45/90]_s$. Clamped boundary condition is assumed for all edges. Table (1) presents the material properties of the composite matrix and SMA fiber [21]. Uniform temperature change was applied to the plate, and the reference temperature is assumed to be 21ºC in this study.

Table 1 Material properties of composite matrix and SMA fiber

Nitinol	Graphite-epoxy
See Fig. 1 and 2 for Young's modulus and recovery stresses. **G** 25.6 GPa **ρ** 6450 Kg/m^3 **ν** 0.3 **α** 10.26×10^{-6} / ºC	**E1** $155\ (1-6.35\times10^{-4}\ \Delta T)$ GPa **E2** $8.07\ (1-7.69\times10^{-4}\ \Delta T)$ GPa **G12** $4.55(1-1.09\times10^{-3}\Delta T)$GPa **ρ** 1550 Kg/m^3 **ν** 0.22 **α1** $-0.07\times10^{-6}(1-0.69\times10^{-3}\Delta T)$ / ºC **α1** $30.6\times10^{-6}(1+0.28\times10^{-4}\Delta T)$ / ºC

Figures (3) and (4) demonstrate the effectiveness of using the SMA-embedded plate to delay the buckling temperature and to reduce the thermal post-buckling deflection. It is seen in the figures that, the increase of volume fraction and pre-strain values of SMA increase the performance of the SMA plate regarding the buckling problem.

Figure (5) presents the effect of changing the value of the dynamic pressure on the post-buckling deflection of a traditional composite plate. It is seen in the figure that the presence of the flow increases the stiffness of the panel, resulting in a lower post-buckling deflection and higher buckling temperature.

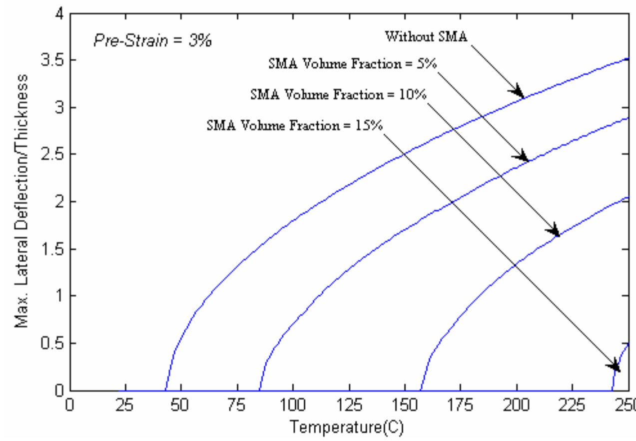

Figure 3 Maximum deflection versus temperature

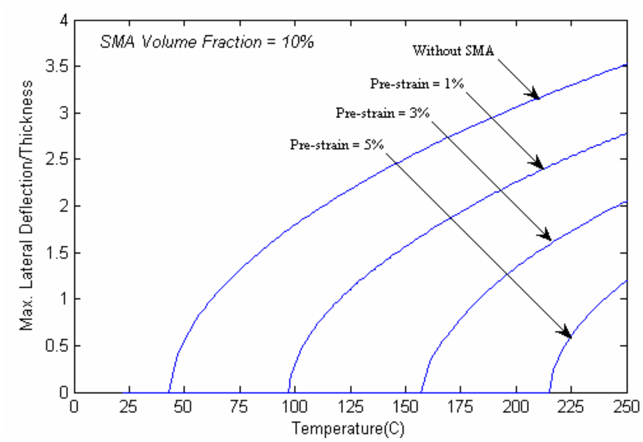

Figure 4 Maximum deflection versus temperature

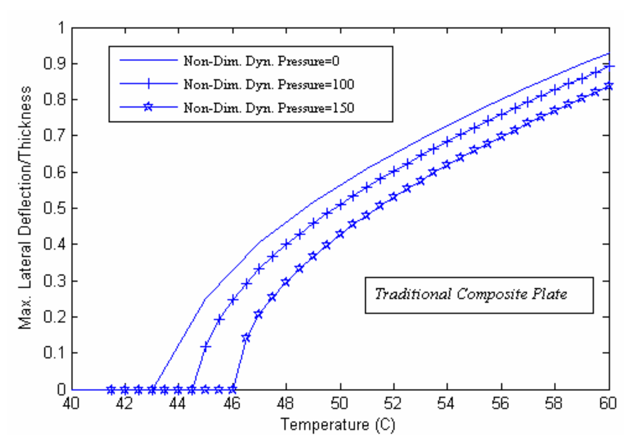

Figure 5 Buckling behavior under aero-thermal loading

4.2. Free Vibration

The vibration characteristics of the laminated composite plate with and without SMA are studied. The material properties, dimensions and stacking sequence of the plate in the vibration analysis are the same as used in section 4.1.

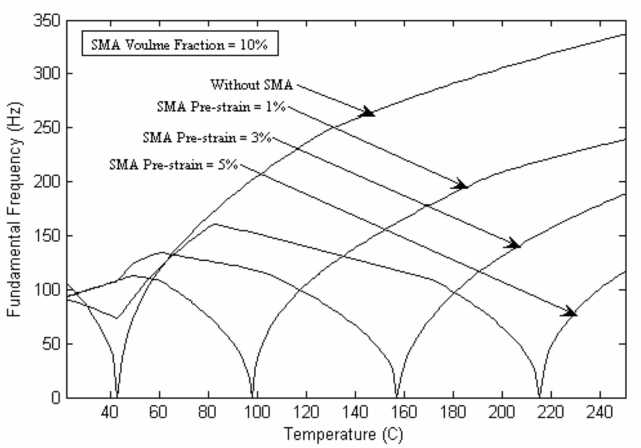

Figure 6 Natural frequencies in the pre-buckled and post-buckled regions

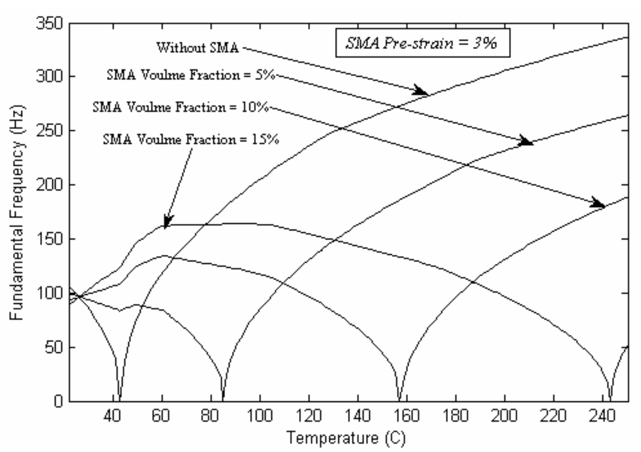

Figure 7 Natural frequencies in the pre-buckled and post-buckled regions

Figures (6) and (7) present the effect of the different volume fractions and pre-strain value on the fundamental frequency of the plate. It is seen in the figures that the first frequency of the plate with and without SMA approach zero as the temperature goes to the critical buckling temperature. In the post-buckling region, the frequencies of the plate with and without SMA increase because the thermal deflection in the post-buckled region increases the nonlinear stiffness matrices. Because of the presence of recovery stress, the frequencies of the plates with SMA are increased first, and then decreased in the pre-buckled region. But, this is not true for the case of 5% volume fraction, as the increase of the thermal forces always overcomes the recovery stress because of the relatively small volume fraction. Also, in the case of 5% pre-strain value, it is seen that the first frequency first decreases in the pre-buckled zone, as the recovery stress increases initially at a slower rate, as shown in figure (2).

4.3. Predicting Panel Flutter Boundaries

In this section, the procedure of determining the critical non-dimensional dynamic pressure under the combined action of aerodynamic and thermal loading is presented.

A traditional clamped composite plate subject to thermal and aerodynamic loading is presented in figure (8) in terms of the critical buckling temperature boundary and linear flutter boundary. The area of the graph is divided into four regions as shown in figure (8). The flat region is where the plate is stable, i.e. neither buckling nor panel flutter occurred. The thermal buckled region is the case in which the thermal stresses overcome the plate stiffness and aerodynamic stiffness. In this region, the plate undergoes static instability. The third region is the flutter region, in which the plate undergoes dynamic instability. The fourth region represents chaos, where thermal buckling and dynamic flutter occur simultaneously. Thus, the wider the flat plate zone is, the more stable is the plate. It is the objective of the SMA fiber embeddings is to increase the flat plate region when the panel is subjected to combined thermal and aerodynamic loading.

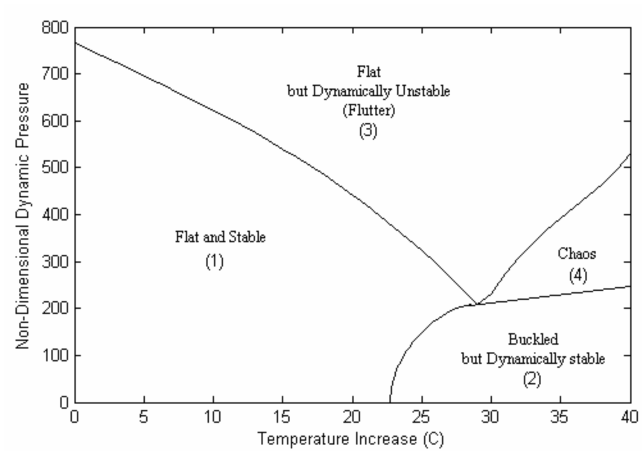

Figure 8 Critical temperature and flutter boundaries

Figures (9) and (10) demonstrate how the recovery stresses with a high volume fraction of SMA overcome the expected decreasing stiffness with temperature increase. Figure 9 illustrates the stability boundary for four different volume fractions with 1% pre-strain value. It is seen in the figure that the higher the volume fraction, the wider the flat and stable region. But, increasing the volume fraction should be optimized, as the SMA fibers are much heavier than the composite matrix.

Figure 10 illustrates the stability boundary for two different pre-strains with 5% volume fraction. It is seen in the figure that the higher the pre-strain value, the wider the flat and stable region. But, it should be noted that the increase in the pre-strain value is bounded by the required fatigue performance of the plate, as high pre-strain values adversely affect the plate fatigue life.

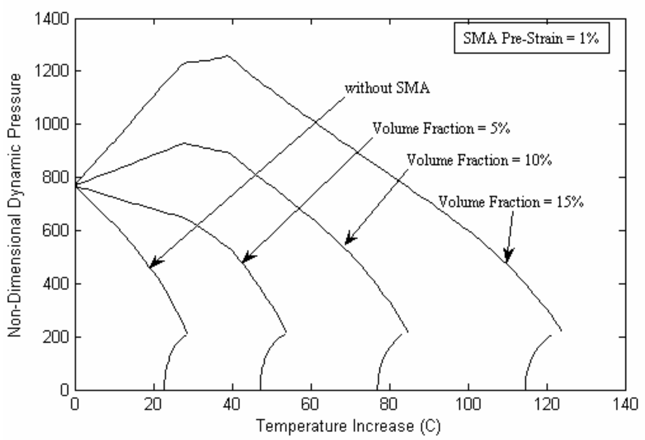

Figure 9 the effectiveness of the SMA plate on the stability boundary for three different volume fractions with 1% pre-strain

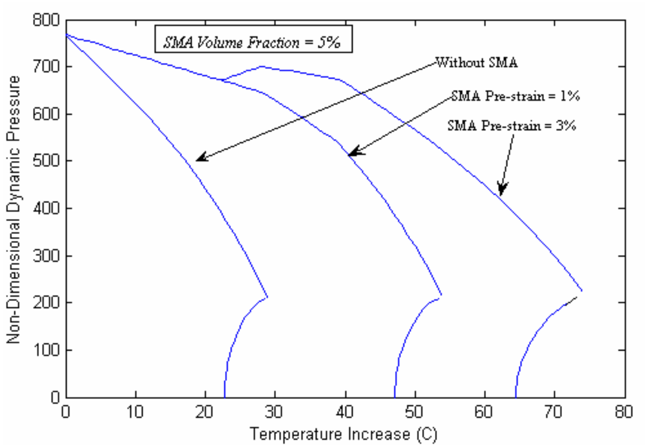

Figure 10 the effectiveness of the SMA plate on the stability boundary for three different volume fractions with 5% volume fraction

5. Conclusions

An efficient finite element formulation based on the first-order shear deformable plate theory was presented for the analysis of supersonic panel flutter and thermal buckling characteristics of SMA hybrid composite plate. Nonlinear temperature-dependent material properties and von Karman moderately large deflection were considered in the formulation. The aerodynamic forces were modeled using the quasi-steady first-order piston theory. The solution procedures of the thermal buckling, free vibration, and panel flutter under thermal loading were presented.

The numerical results of this study demonstrate a significant increase in the buckling temperature and a noteworthy reduction in the post buckling deflection of the SMA-embedded plate. The combined aerodynamic-thermal loading problem was investigated as well in order to determine the effectiveness of SMA-embedded plates in increasing the flutter stability boundaries. The critical non-dimensional dynamic pressure has shown significant increase for the SMA-embedded plates. The effectiveness of SMA volume fractions and pre-strain values has also been investigated.

In spite of the increase of the weight of the plate and decrease of the thermal large deflection using the SMA fibers, in the pre-buckling region, the natural frequencies can be increased due to the recovery stress of the SMA fibers. However, in the post-buckled region, the natural frequencies of the plate with SMA are lower than those of the plate without SMA. This is due to the decrease of the post-buckling deflection and hence the decrease in the nonlinear stiffness terms caused by the SMA recovery stresses.

Therefore, SMA can be useful to the application of the structures due to their controllability of the natural frequency, thermal deflection and flutter boundaries.

References

[1] Tauchart T. R., 1991, “Thermally induced flexure, buckling, and vibration of plates”, Appl. Mech. Rev., Vol. 44, no. 8.

[2] Thornton E. A., 1993, “Thermal buckling of plates and shells”, Appl. Mech. Rev., Vol. 46, no. 10, pp. 485-506.

[3] Shi Y., and Mei, C., 1999,” Thermal post-buckling of composite plates using the finite element modal coordinate method”, AIAA, 1467-CP, pp. 1355-1362.

[4] Gray, C. C., and Mei, C., 1991,”Finite element analysis of thermal post-buckling and vibrations of thermally buckled composite plates”, AIAA, 1239-CP, pp. 2996-3007.

[5] Jones, R., and Mazumdar , J., 1980, “Vibration and buckling of plates at elevated temperatures”, International Journal of solid Structures, Vol. 16, pp. 61-70.

[6] Shi, Y., Lee, R. Y., and Mei, C., 1999, “Coexiting thermal post-buckling of composite plates with initial imperfections using finite element modal method”, Journal of Thermal stresses, Vol. 22, pp. 595-614.

[7] Joradan, P. F., 1956, "The Physical Nature of Panel Flutter", Aero Digest, pp. 34-38.

[8] Mei C., Abdel-Motagaly, K., and Chen, R., 1999, "Review of nonlinear panel flutter at supersonic and hypersonic speeds", Appl. Mech. Rev., 52 (10), pp. 321-332.

[9] Liaw, D. G., 1997, "Nonlinear Supersonic Flutter of Laminated Composite Plates under Thermal Loads”, Computers & Structures, 65 (5), pp. 733-740.

[10] Abdel-Motagaly, K., Chen, R., and Mei, C., 1999, "Effects of Flow Angularity on Nonlinear Supersonic Flutter of Composite Panels Using Finite Element Method", 40th Structure, Structural Dyn. and Mat. Conf., St louis MO, pp. 1963-1972.

[11] Mei, C., 1977, "A Finite-Element Approach for Nonlinear Panel Flutter", AIAA Journal, 15 (8), pp. 1107-1110.

[12] Dixon, I. R. and Mei, C., 1993, "Finite Element Analysis of Large-Amplitude Panel Flutter of Thin Laminates", AIAA Journal, 31 (4), pp. 701-707.

[13] Xue D. Y. and Mei, C., 1993, "Finite Element Nonlinear Panel Flutter with Arbitrary Temperatures in Supersonic Flow", AIAA Journal, 31 (1), pp. 154-162.

[14] Sarma, B. S. and Varadan, T. K., "Nonlinear Panel Flutter By Finite Element Method", AIAA Journal, 1987, 26 (5), pp. 566-574.

[15] Dongi, F., Dinkler, D., and Kroplin , B., 1996,"Active Panel Flutter Suppression Using Self-Sensing Piezoactuators", AIAA Journal, 34 (6), pp. 1224-1230.

[16] Lee, I., Jin, H., and Oh, II-Kown, 2003, "Aerothermoelastic Phenomena of Aerospace and Composite Structures", Journal of Thermal Stresses, 23, pp. 525-546.
[17] Cross, W.B, Kariotis, A. H., Stimeler, F. J., 1969,"Nitinol characterization study", NASA CR-14B.
[18] Birman, V., 1997,"Review of Mechanics of Shape Memory Alloy Structures", Appl. Mech. Rev., 50, pp. 629-645.
[19] Jia, J., and Rogers, C. A., 1992, "Formulation of a mechanical model for composites with embedded SMA actuators", Journal of Mechanical Design, Vol. 114, pp. 670-676.
[20] Park, J. S., Kim, J. H., and Moon, S. H., 2004, "Vibration of Thermally Post-Buckled Composite Plates Embedded with Shape Memory Alloy Fibers", Composite Structures, 63, pp. 179-188.
[21] Guo, X., 2005, "Shape Memory Alloy Applications on Control of Thermal Buckling, Panel Flutter and Random Vibration of Composite Panels", PhD dissertation, Old Dominion University, Mechanical Engineering Department, Norfolk, Virginia.
[22] Tawfik, M., Ro, J. J., and Mei, C., 2002, "Thermal Post-Buckling and Aeroelastic Behavior of Shape Memory Alloy Reinforced Plates", Smart Materials and Structures, 11, pp. 297-307.
[23] Duan, B., Tawfik, M., Goek, S., Ro, J. J., and Mei, C, 2000, " Analysis and Control of Large Thermal Deflection of Composite Plates Using Shape Memory Alloy", Industrial and Commercial Applications of Smart Structures, SPIE, Vol. 3991, pp. 358-365.
[24] Roh, J. H., Oh , I. K., Yang , S.H., Han , J. H. and Lee, I., 2004, " Thermal Post-Buckling Analysis of Shape Memory Alloy Hybrid Composite Shell Panels", Smart Material and Structures, Vol. 13, pp. 1337-1344.
[25] Brinson, L. C. and Lammering , R., 2004, "Finite Element Analysis of the Behavior of Shape Memory Alloys and their Applications", International Journal of Solids and Structures, Vol.30, 2004, pp. 3261-3280.
[26] Gilat, R, and Aboudi, J., 2004, "Dynamic Response of Active Composite Plates: Shape Memory Alloy Fibers in Polymeric/Metallic Matrices", International Journal of Solids and Structures; Vol. 41, pp. 5717-5731.
[27] GUO, X., Przckop, A. and Mei, C., 2005,"Supersonic Nonlinear Panel flutter suppression using Aeroelastic Modes and Shape Memory Alloys". 46th AIAA/ASME/ASCE/AHS/ASC Structures, Structural Dynamics and Material Conference, Austin, Texas.
[28] Xue, D. Y., , 1991"Finite Element Frequency Domain Solution of Nonlinear Panel Flutter with Temperature Effects and Fatigue Life Analysis", PhD dissertation, Old Dominion University, Mechanical Engineering Department, Norfolk, Virginia.